

Power-Based Generation Expansion Planning for Flexibility Requirements

Diego A. Tejada-Arango ^{id}, *Member, IEEE*, Germán Morales-España ^{id}, *Senior Member, IEEE*,
Sonja Wogrin ^{id}, *Senior Member, IEEE*, and Efraim Centeno ^{id}

Abstract—Flexibility requirements are becoming more relevant in power system planning due to the integration of variable Renewable Energy Sources (vRES). In order to consider these requirements Generation Expansion Planning (GEP) models have recently incorporated Unit Commitment (UC) constraints, using traditional energy-based formulations. However, recent studies have shown that energy-based UC formulations overestimate the actual flexibility of the system. Instead, power-based UC models overcome these problems by correctly modeling ramping constraints and operating reserves. This paper proposes a power-based GEP-UC model that improves the existing models. The proposed model optimizes investment decisions on vRES, Energy Storage Systems (ESS), and thermal technologies. In addition, it includes real-time flexibility requirements, and the flexibility provided by ESS, as well as other UC constraints, e.g., minimum up/down times, startup and shutdown power trajectories, network constraints. The results show that power-based model uses the installed investments more effectively than the energy-based models because it more accurately represents flexibility capabilities and system requirements. For instance, the power-based model obtains less investment (6–12%) and yet it uses more efficiently this investment because operating cost is also lower (2–8%) in a real-time validation. We also propose a semi-relaxed power-based GEP-UC model, which is at least 10 times faster than its full-integer version and without significantly losing accuracy in the results (less than 0.2% error).

Index Terms—Generation expansion planning, unit commitment, energy storage systems, capacity expansion planning, power system planning, power generation planning.

NOMENCLATURE

A. Indices and sets

- $j \in \mathcal{J}$ Technologies.
 $g \in \mathcal{G} \subseteq \mathcal{J}$ Subset of thermal generation technologies.
 $v \in \mathcal{V} \subseteq \mathcal{J}$ Subset of renewable energy sources.

Manuscript received February 20, 2019; revised June 9, 2019 and August 30, 2019; accepted September 6, 2019. Date of publication October 15, 2019; date of current version April 22, 2020. This work was partially supported by Project Grant ENE2016-79517-R, awarded by the Spanish Ministerio de Economía y Competitividad; and projects 060.33957 and 060.38253, founded by TNO's internal R&D. Paper no. TPWRS-00254-2019.R2. (*Corresponding author: Diego A. Tejada-Arango.*)

D. A. Tejada-Arango, S. Wogrin, and E. Centeno are with the Universidad Pontificia Comillas, ICAI, Instituto de Investigación Tecnológica, 28015 Madrid, Spain (e-mail: dtejada@comillas.edu; swogrin@comillas.edu; efrain@comillas.edu).

G. Morales-España is with the Energy Transition Studies, ECN part of TNO, 1043 NT Amsterdam, The Netherlands (e-mail: german.morales@tno.nl).

Color versions of one or more of the figures in this article are available online at <http://ieeexplore.ieee.org>.

Digital Object Identifier 10.1109/TPWRS.2019.2940286

- $s \in \mathcal{S} \subseteq \mathcal{J}$ Subset of energy storage technologies.
 $b \in \mathcal{B}$ Buses.
 $\mathcal{B}^D \subseteq \mathcal{B}$ Subset of buses b with demand consumption.
 $l \in \mathcal{L}$ Transmission lines.
 $\omega \in \Omega$ Scenarios.
 $k \in \mathcal{K}_g$ Startup segments, running from 1 (the hottest) to K_g (the coldest).
 $t \in \mathcal{T}$ time periods (e.g., hours).

B. Parameters

- C_j^I Technology investment cost [\$/MW].
 C_j^{LV} Linear variable production cost [\$/MWh].
 C_g^{NL} No-load cost [\$/h].
 C_g^{SD} Shutdown cost [\$/].
 C_{gk}^{SU} Startup cost for segment k [\$/].
 C_g^{EM} CO2 emission cost [\$/MWh].
 C_j^{R+}, C_j^{R-} Up/down reserve cost [\$/MW].
 $D_{\omega bt}^E$ Energy demand on bus b [MWh].
 $D_{\omega bt}^P$ Power demand on bus b [MW].
 $R_{\omega t}^+, R_{\omega t}^-$ Up/down reserve requirement [MW].
 \bar{F}_l Power flow limit on transmission line l [MW].
 $\bar{P}_g, \underline{P}_g$ Maximum/minimum power output [MW].
 $E_{gkt}^{SU}, E_{gt}^{SD}$ Energy output during startup/shutdown [MWh].
 $P_{gkt}^{SU}, P_{gt}^{SD}$ Power output during startup/shutdown [MW].
 RU_g, RD_g Ramp-up/down capability [MW/min].
 RU_s, RD_s Ramp-up/down capability [(MW/min)/MW].
 SU_g, SD_g Startup/shutdown capability [MW].
 SU_g^D, SD_g^D Startup/shutdown duration [h].
 T_{gk}^{SU} Time interval limit of startup segment k [h].
 TU_g, TD_g Minimum up/down time [h].
 $\Gamma_{lj}^J, \Gamma_{lb}$ Shift factors for line l [p.u.].
 EPR_s Energy to power ratio [h].
 $V_{\omega vt}^E$ Renewable energy output profile [p.u.].
 $V_{\omega vt}^P$ Renewable power output profile [p.u.].
 π_ω Probability of scenario ω .
 \bar{X}_j Investment limit for technology j .
 X_j^0 Initial capacity for technology j ; [# units] for g , and [MW] for s and v .

C. Continuous non-negative variables

- $\hat{e}_{\omega jt}$ Total energy output in time t [MWh].
 $\hat{p}_{\omega jt}$ Total power output at the end of time t [MW].
 $e_{\omega jt}$ Energy output above minimum output in time t [MWh].

$p_{\omega gt}$	Power output above minimum output at the end of time t [MW].
$\hat{c}_{\omega st}$	Charged energy for storage in time t [MWh].
$c_{\omega st}$	Charged power for storage at the end of time t [MW].
$r_{\omega gt}^+$	Up capacity reserve in time t [MW].
$r_{\omega gt}^-$	Down capacity reserve in time t [MW].
$\phi_{\omega st}$	Energy storage level in time t [MWh].

D. Integer Variables

$u_{\omega gt}$	Unit commitment for thermal technologies.
$y_{\omega gt}$	Startup for thermal technologies.
$z_{\omega gt}$	Shutdown for thermal technologies.
$\delta_{\omega gkt}$	Startup type selection for thermal technologies.
$\gamma_{\omega st}$	Binary decision for charging/discharging logic.
x_j	Investment decision per technology.

I. INTRODUCTION

GENERATION Expansion Planning (GEP) is a classic long-term problem in power systems that aims at determining the optimal generation technology mix [1]. Environmental policies, such as renewable targets [2] or CO₂ emission reduction [3] influence in GEP decisions, leading to the integration of vast amounts of variable Renewable Energy Sources (vRES), i.e., wind and solar, in GEP. Nevertheless, vRES integration has consequences in GEP modeling. For instance, previous studies [4]–[6] have shown the importance of including short-term dynamics on GEP decisions in order to consider the increased need of operational flexibility due to vRES integration. Therefore, correctly modeling flexibility in GEP models is crucial to reach the right conclusions in the energy transition process.

In order to consider operational flexibility in GEP, Unit Commitment (UC) modeling is needed to determine system operation [6], [7]. For example, it is known that units are being cycled more frequently due to higher vRES flexibility requirements [8]. Studies have shown that ignoring startup and shutdown processes highly overestimates the flexibility and costs of the system [9]. Another example is ramping constraints. If we focus on flexibility and want to know a good (optimal) future generation-mix and interconnection capacities for a given scenario, the GEP problem must include at least detailed ramping constraints. Moreover, operating reserve decisions have also become more relevant in GEP with the integration of vRES because they may ensure that generation technologies have an extra income to recover their investment costs through these types of ancillary services.

Despite the recent developments to consider flexibility requirements in GEP, classic GEP models use energy-based formulations, such as TIMES modeling framework [10], the Regional Energy Deployment System (ReEDS) framework [11], Resource Planning Model (RPM) [12], and COMPETES [13]. Recent studies [9], [14], [15] have shown that energy-based UC models cannot capture variability on demand and vRES, and even assuming that they capture it, they cannot deliver the flexibility that they promise, that is, they intrinsically and hiddenly overestimate the flexibility of the system. In addition,

energy-based formulations inherently lead unfeasible ramping constraints as widely discussed in the literature [16], [17]. This is mainly because average energy levels (e.g., average level in one hour) do not provide detailed information about the instantaneous output of a generator, and constraints such as ramping-limits and demand-balance are dependent on instantaneous outputs rather than average levels. This means that more flexibility than planned by energy-based models is used in real-time operation (through operating reserves and allowing deviations on schedules) to deal with all the problems introduced by these traditional energy-based models. These problems are hidden in the formulations, and to assess really their performance, real-time simulations are required (e.g., 5-min dispatch), as it is widely discussed in [9].

More recently, power-based models have been proposed [14], [18] to overcome these problems by better exploiting the system flexibility [9], by allowing the correct modeling of ramping constraints and operating reserves [14], [15] in order to deliver the expected and actual flexibility from the generation resources. This is possible because a power-based model has a clear distinction between power and energy in its core formulation. Demand and generation are modeled as hourly piecewise-linear functions representing their instantaneous power trajectories. The schedule of a generating unit output is no longer an energy stepwise function, but a smoother piece-wise power function.

Another important aspect to determine the flexibility requirements in power systems is time resolution. In order to model correctly the real operation of power systems a high resolution is needed (e.g., minutes). Current GEP models are based on hourly resolution where the underlying assumption is that it is enough to capture the variability and flexibility requirements of power systems. However, it has already been shown in [9] that real-time simulations (e.g., 5-min time step) help to determine the performance of different schedules (operational decisions) to meet the real-time flexibility requirements in the power system. This type of real-time validation is not common to be carried out because it is considered unnecessary. Nevertheless, to validate correctly flexibility capabilities and requirements of the system, this real-time evaluation is paramount [9]. Therefore, we carry out a real-time validation stage (e.g., 5-min simulation) in order to evaluate the quality of investment and operational decisions obtained with the models that have been analyzed in this paper.

In this paper, we propose a novel power-based model for GEP presenting advantages over the traditional energy-based models. The proposed model optimizes investment decisions on vRES, Energy Storage Systems (ESS), and thermal technologies. ESS are included because they represent one of the most promising options to provide flexibility in power systems in the future [19]. In addition, the investment and operational decisions are tested in a real-time validation stage to better reflect the actual flexibility that these decisions can provide. The main contributions of this paper are as follows:

- 1) This paper proposes an investment decision model for generation and energy storage technologies using a power-based UC formulation as an extension of the classic energy-based UC formulations. The proposed power-based GEP-UC model improves the classic energy-based

long-term capacity expansion models by representing the flexibility requirements of power systems more accurately (i.e., reserve decisions and ramping constraints) in a long-term horizon considering investment decisions. Moreover, we also propose a novel power-based formulation for ESS (e.g., batteries), so it can be included in the proposed power-based model for operation and investment decisions. It is important to highlight that both the power-based GEP-UC and the power-based ESS modeling for investment and operation represent original contributions as they have not been proposed in the literature before.

- 2) In order to improve how this extended problem can be addressed, we also propose a semi-relaxed version of the power-based GEP-UC model, which aims at reducing the computational burden without losing accuracy in the results. In fact, the real-time validation stage shows that this semi-relaxed version performs better than the classic energy-based (integer) model, i.e., makes investment and operation decisions that lead to lower costs and emissions than those obtained by short-term models, while also solving considerably faster. To the authors' knowledge, this type of insight has not been obtained before in the literature.

The paper is organized as follows: Section II shows model formulations used for the GEP problem, considering both energy- and power-based equations. Section 0 explains the procedure to evaluate the power system flexibility. Section 0 summarizes the data of each case study. Section V discusses the main results, including a sensitivity analysis to the ramp capacity of the generation units. Finally, Section VI concludes this paper.

II. GENERATION EXPANSION MODEL FORMULATIONS

This section presents the objective function and set of constraints for the energy- and the power-based GEP-UC formulations. These constraints include investment decisions for different generation technologies: thermal generation, ESS, and vRES.

Before presenting and discussing the energy- and power-based model formulations, let us briefly comment on input data of the respective models. As indicated by the model name, in the power-based model most of the constraints are represented in terms of power, whereas their equivalent in the energy-based model is formulated in terms of energy. As a consequence, a power-based model requires power data (e.g., in MW units), and energy-based models require energy data (e.g., in MWh units). While the actual input data might be different in type and units, it stems from the same original data, which makes the model comparison fair. For example, consider the demand curve given in Fig. 1. The energy-based model uses data corresponding to energy blocks (as given by the blue step function), whereas the power-based model uses data representing a power trajectory (as given by the orange piecewise linear curve). It is important to highlight that the total energy in both models is the same. However, decision variables and constraints change depending on whether we optimize the energy- or the power-based model,

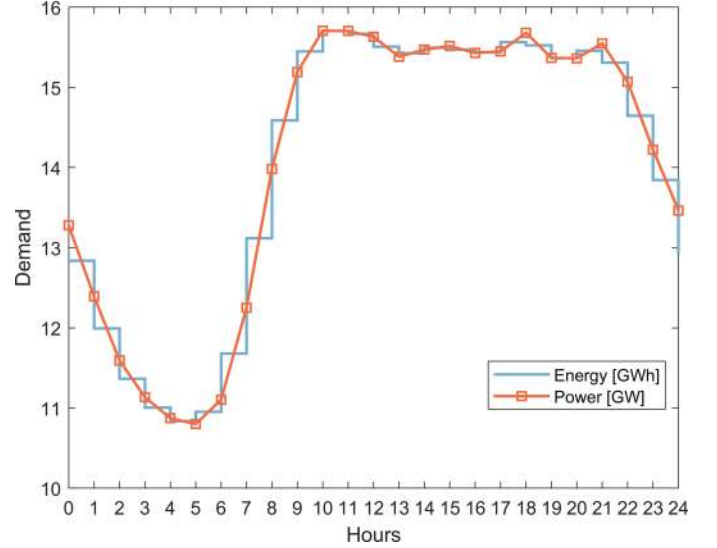


Fig. 1. Power demand trajectory and hourly energy demand.

as we show in the following sections. Please note that similar transformations occur for vRES time series.

Finally, operational decisions are considered using a clustered UC formulation (i.e., aggregating similar generating units into one group or cluster), which is commonly applied in long-term planning models [7], [20], [21].

A. Energy-Based Formulation

The GEP seeks to minimize the investment costs plus the expected value of operating costs: production cost, up/down reserve cost, CO2 emission cost, no-load cost, shutdown cost, startup cost. Notice that $\Psi = \{x, e, \hat{e}, \hat{c}, r^+, r^-, u, y, z, \delta, \phi\}$ corresponds to the set of decision variables considered in this model.

$$\begin{aligned} \min_{\Psi} & \sum_{j \in \mathcal{J}} C_j^I x_j + \sum_{\omega \in \Omega} \pi_{\omega} \sum_{t \in \mathcal{T}} \left\{ \sum_{j \in \mathcal{J}} \left[C_j^{LV} \hat{e}_{\omega jt} \right. \right. \\ & + C_j^{R+} r_{\omega jt}^+ + C_j^{R-} r_{\omega jt}^- \left. \right] + \sum_{g \in \mathcal{G}} \left[C_g^{EM} \hat{e}_{\omega gt} + C_g^{NL} u_{\omega gt} \right. \\ & \left. \left. + C_g^{SD} z_{\omega gt} + \sum_{k \in \mathcal{K}_g} C_{gk}^{SU} \delta_{\omega gkt} \right] \right\} \end{aligned} \quad (1)$$

The system-wide constraints are guaranteed by energy demand balance (2), transmission limits (3), and reserve requirements (4)–(5):

$$\sum_{j \in \mathcal{J}} \hat{e}_{\omega jt} - \sum_{s \in \mathcal{S}} \hat{c}_{\omega st} = \sum_{b \in \mathcal{B}^D} D_{\omega bt}^E \quad \forall \omega, t \quad (2)$$

$$-\bar{F}_l \leq \sum_{j \in \mathcal{J}} \Gamma_{lj}^J \hat{e}_{\omega jt} - \sum_{s \in \mathcal{S}} \Gamma_{ls}^S c_{\omega st} - \sum_{b \in \mathcal{B}^D} \Gamma_{lb} D_{\omega bt}^E \leq \bar{F}_l \quad (3)$$

$$\forall l, \omega, t$$

$$\sum_{j \in \mathcal{J}} r_{\omega jt}^+ \geq R_{\omega t}^+ \quad \forall \omega, t \quad (4)$$

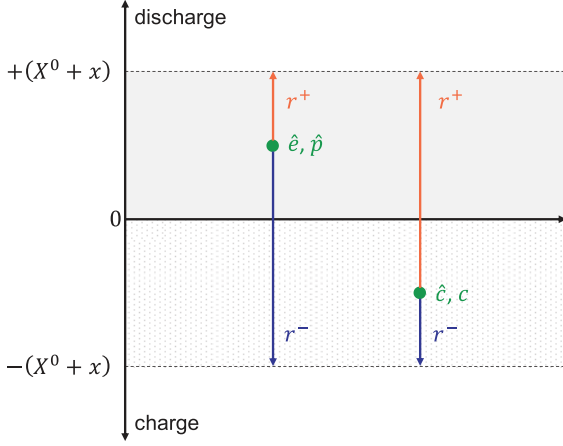


Fig. 2. ESS providing reserves from different operation points.

$$\sum_{j \in \mathcal{J}} r_{\omega jt}^- \geq R_{\omega t}^- \quad \forall \omega, t \quad (5)$$

The relationship between operational and investment decisions for each technology type is guaranteed with (6) for thermal technologies, (7), (8) for ESS, and (9) for vRES. Notice that (7), (8) model the reserve variables that ESS can provide whether the ESS is charging or discharging, see Fig. 2. These constraints define the flexibility reserves that ESS can provide.

$$u_{\omega gt} \leq X_g^0 + x_g \quad \forall \omega, g, t \quad (6)$$

$$\hat{e}_{\omega st} - \hat{c}_{\omega st} + r_{\omega gt}^+ \leq X_s^0 + x_s \quad \forall \omega, s, t \quad (7)$$

$$\hat{e}_{\omega st} - \hat{c}_{\omega st} - r_{\omega gt}^- \geq -(X_s^0 + x_s) \quad \forall \omega, s, t \quad (8)$$

$$\hat{e}_{\omega vt} \leq V_{\omega vt}^E (X_v^0 + x_v) \quad \forall \omega, v, t \quad (9)$$

Thermal generation constraints include: commitment/ startup/ shutdown logic (10), minimum up/down times (11), (12), startup type selection (13), (14) (e.g., hot, warm, and cold startup), energy production limits including reserve decisions (15)–(18) (where \mathcal{G}^1 is defined as the thermal technologies in \mathcal{G} with $TU_g = 1$), and total energy production (19). The UC formulation presented here is based on the tight and compact formulation proposed in [22]. Furthermore, Gentile *et al.* [23] have proven that the set of constraints (10)–(12) together with (15)–(19) is the tightest representation (i.e., convex hull) for the energy-based model.

$$u_{\omega gt} - u_{\omega g, t-1} = y_{\omega gt} - z_{\omega gt} \quad \forall \omega, g, t \quad (10)$$

$$\sum_{i=t-TU_g+1}^t y_{\omega gi} \leq u_{\omega gt} \quad \forall \omega, g, t \in [TU_g, T] \quad (11)$$

$$\sum_{i=t-TD_g+1}^t z_{\omega gi} \leq (X_g^0 + x_g) - u_{\omega gt} \quad \forall \omega, g, t \in [TD_g, T] \quad (12)$$

$$\delta_{\omega gkt} \leq \sum_{i=T_g^{SU}}^{T_g^{SU}-1} z_{\omega g, t-i} \quad \forall \omega, g, k \in [1, K_g], t \quad (13)$$

$$\sum_{k \in K_g} \delta_{\omega gkt} = y_{\omega gt} \quad \forall \omega, g, t \quad (14)$$

$$e_{\omega gt} + r_{\omega gt}^+ \leq (\bar{P}_g - \underline{P}_g) u_{\omega gt} - (\bar{P}_g - SD_g) z_{\omega g, t+1} - \max(SD_g - SU_g, 0) y_{\omega gt} \quad \forall \omega, g \in \mathcal{G}^1, t \quad (15)$$

$$e_{\omega gt} + r_{\omega gt}^+ \leq (\bar{P}_g - \underline{P}_g) u_{\omega gt} - (\bar{P}_g - SU_g) y_{\omega g, t} - \max(SU_g - SD_g, 0) z_{\omega g, t+1} \quad \forall \omega, g \in \mathcal{G}^1, t \quad (16)$$

$$e_{\omega gt} + r_{\omega gt}^+ \leq (\bar{P}_g - \underline{P}_g) u_{\omega gt} - (\bar{P}_g - SU_g) y_{\omega g, t} - (\bar{P}_g - SD_g) z_{\omega g, t+1} \quad \forall \omega, g \notin \mathcal{G}^1, t \quad (17)$$

$$e_{\omega gt} - r_{\omega gt}^- \geq 0 \quad \forall \omega, g, t \quad (18)$$

$$\hat{e}_{\omega gt} = \underline{P}_g u_{\omega gt} + e_{\omega gt} \quad \forall \omega, g, t \quad (19)$$

Traditional energy-based UC formulations ignore the inherent startup (SU) and shutdown (SD) trajectories of thermal generation, assuming they start/end their production at their minimum output. Authors in [9], [14] have shown the relevance of the SU and SD processes when they are included in the scheduling optimization. Therefore, we also analyze the energy-based formulation including the SU/SD trajectories proposed in [24]. Thus, if SU/SD trajectories are considered then (19) is replaced by (20).

$$\hat{e}_{\omega gt} = \underbrace{\sum_{k=1}^{K_g} \sum_{i=1}^{SU_g^D} E_{gki}^{SU} \delta_{\omega gk, (t-i+SU_g^D+1)}}_{\text{Startup trajectory}} + \underbrace{\sum_{i=1}^{SD_g^D} E_{gi}^{SD} z_{\omega g, (t-i+1)}}_{\text{Shutdown trajectory}} + \underbrace{\underline{P}_g u_{\omega gt} + e_{\omega gt}}_{\text{Output when being up}} \quad \forall \omega, g, t \quad (20)$$

ESS constraints include: logic to avoid charging and discharging at the same time (21), (22), the definition of the storage inventory level (23), storage limits including reserve (24), (25). Since ESS can provide reserves (Fig. 2), the binary variable $\gamma_{\omega st}$ in (21), (22) guarantees that the ESS is only charging or discharging at time period t . Without (21), (22), the optimization model could find a non-realistic solution where the ESS is charging and discharging simultaneously in order to provide more reserves from the ESS.

$$\hat{c}_{\omega st} \leq (1 - \gamma_{\omega st}) \cdot (X_s^0 + \bar{X}_s) \quad \forall \omega, s, t \quad (21)$$

$$\hat{e}_{\omega st} \leq \gamma_{\omega st} \cdot (X_s^0 + \bar{X}_s) \quad \forall \omega, s, t \quad (22)$$

$$\phi_{\omega st} = \phi_{\omega s, t-1} + \eta_s \hat{c}_{\omega st} - \hat{e}_{\omega st} \quad \forall \omega, s, t \quad (23)$$

$$\phi_{\omega st} \leq EPR_s (X_s^0 + x_s) - \sum_{i=t-1}^t r_{\omega gi}^- \quad \forall \omega, s, t \quad (24)$$

$$\phi_{\omega st} \geq \sum_{i=t-1}^t r_{\omega gi}^+ \quad \forall \omega, s, t \quad (25)$$

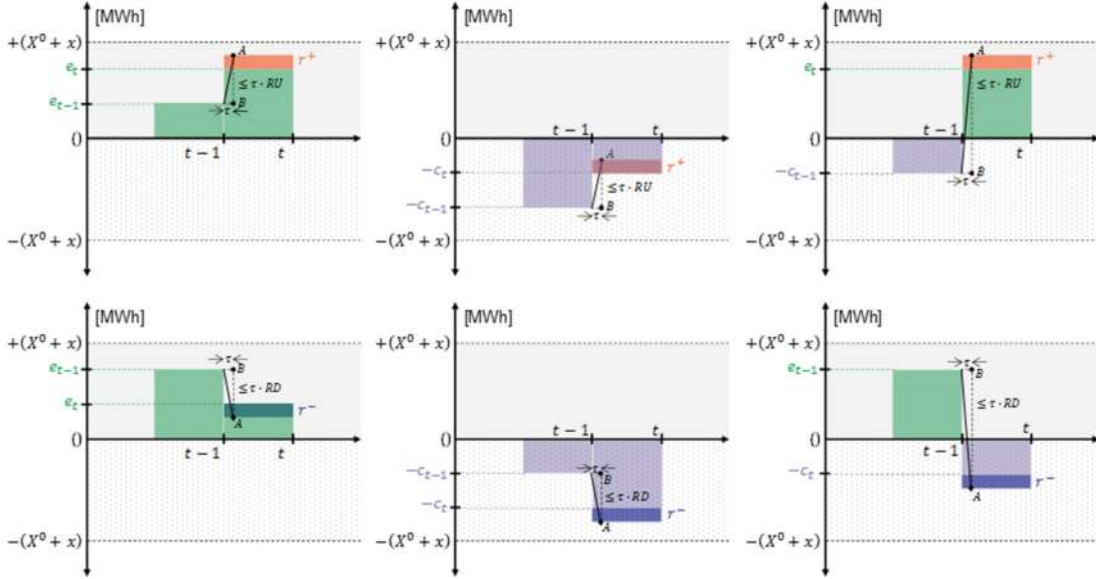


Fig. 3. Ramping constraints for ESS in the energy-based model.

Flexibility requirements in the power system are represented by ramping constraints including reserve decisions. In order to guarantee that scheduled reserves are feasible to provide at τ -min (e.g., $\tau = 5$) using the energy-based formulation, it is necessary to consider the ramping capability at τ -min. For instance, ramp capability limits imposed with (26), (27) consider the reserve that thermal technologies can provide at τ -min. ESS ramp capability limits (28), (29) consider the charged energy in addition to the energy output (i.e., discharged energy), as in [25]. Fig. 3 shows the ramping constraints for ESS in the energy-based model for all possible operational conditions of the ESS going from time period $t - 1$ to t . Notice that (28), (29) allow ESS to switch from charging to discharging within the ramp limit, i.e., segment AB in Fig. 3.

$$(e_{\omega g t} - e_{\omega g, t-1}) + r_{\omega g t}^+ \leq \tau R U_g u_{\omega g t} \quad \forall \omega, g, t \quad (26)$$

$$-(e_{\omega g t} - e_{\omega g, t-1}) + r_{\omega g t}^- \leq \tau R D_g u_{\omega g, t-1} \quad \forall \omega, g, t \quad (27)$$

$$(\hat{e}_{\omega s t} - \hat{e}_{\omega s, t-1}) - (\hat{c}_{\omega s t} - \hat{c}_{\omega s, t-1}) + r_{\omega s t}^+ \leq \tau R U_s (X_s^0 + x_s) \quad \forall \omega, s, t \quad (28)$$

$$(\hat{c}_{\omega s t} - \hat{c}_{\omega s, t-1}) - (\hat{e}_{\omega s t} - \hat{e}_{\omega s, t-1}) + r_{\omega s t}^- \leq \tau R D_s (X_s^0 + x_s) \quad \forall \omega, s, t \quad (29)$$

B. Power-Based Formulation

This section shows the GEP-UC equations in terms of power. However, some of the terms in these equations are naturally linked to energy. For instance, the objective function (30) includes the so-called calculated energy $\hat{e}_{\omega j t}$ to obtain the variable cost and CO2 emission cost. Equation (31) determines the energy output from the power output variables $\hat{p}_{\omega j t}$. Since the variable and CO2 costs are intrinsically based on energy, energy variables are then used in the objective function for both power-

and energy-based models. In addition, for ESS the charged energy $\hat{c}_{\omega s t}$ is also determined using the charged power in (32). Notice that $\Lambda = \{x, p, \hat{p}, \hat{e}, c, \hat{c}, r^+, r^-, u, y, z, \delta, \phi\}$ corresponds to the set of decision variables in this model.

$$\begin{aligned} \min_{\Lambda} \sum_{j \in \mathcal{J}} C_j^I x_j + \sum_{\omega \in \Omega} \pi_{\omega} \sum_{t \in \mathcal{T}} \left\{ \sum_{j \in \mathcal{J}} \left[C_j^{LV} \hat{e}_{\omega j t} \right. \right. \\ \left. \left. + C_j^{R+} r_{\omega j t}^+ + C_j^{R-} r_{\omega j t}^- \right] + \sum_{g \in \mathcal{G}} \left[C_g^{EM} \hat{e}_{\omega g t} + C_g^{NL} u_{\omega g t} \right. \right. \\ \left. \left. + C_g^{SD} z_{\omega g t} + \sum_{k \in \mathcal{K}_g} C_{gk}^{SU} \delta_{\omega g k t} \right] \right\} \quad (30) \end{aligned}$$

$$\hat{e}_{\omega j t} = \frac{\hat{p}_{\omega j t} + \hat{p}_{\omega j, t-1}}{2} \quad \forall \omega, j, t \quad (31)$$

$$\hat{c}_{\omega s t} = \frac{c_{\omega s t} + c_{\omega s, t-1}}{2} \quad \forall \omega, s, t \quad (32)$$

Demand balance constraint (33) and power-flow transmission limits (34) also use the power output instead of energy output. The power trajectories, e.g., $D_{\omega b t}^P$ for demand, can be obtained and forecasted using the system operator real-time data. Then, the hourly energy can be calculated from the power trajectory using the area under the curve. Ref. [26] shows the relation between energy and power schedules. Reserve requirements (4), (5) remain the same because they are already expressed in terms of power.

$$\sum_{j \in \mathcal{J}} \hat{p}_{\omega j t} - \sum_{s \in \mathcal{S}} c_{\omega s t} = \sum_{b \in \mathcal{B}^D} D_{\omega b t}^P \quad \forall \omega, t \quad (33)$$

$$\begin{aligned} -\bar{F}_l \leq \sum_{j \in \mathcal{J}} \Gamma_{lj}^J \hat{p}_{\omega j t} - \sum_{s \in \mathcal{S}} \Gamma_{ls}^S c_{\omega s t} - \sum_{b \in \mathcal{B}^D} \Gamma_{lb} D_{\omega b t}^P \\ \leq \bar{F}_l \quad \forall l, \omega, t \quad (34) \end{aligned}$$

In terms of the relationship between operational and investment decisions, thermal unit constraint (6) remains the same. However, constraints for ESS and vRES technologies change to (35), (36) and (37), respectively. As in the energy-based model, (35), (36) consider reserve variables, see Fig. 2.

$$\hat{p}_{\omega st} - c_{\omega st} + r_{\omega gt}^+ \leq X_s^0 + x_s \quad \forall \omega, s, t \quad (35)$$

$$\hat{p}_{\omega st} - c_{\omega st} - r_{\omega gt}^- \geq -(X_s^0 + x_s) \quad \forall \omega, s, t \quad (36)$$

$$\hat{p}_{\omega vt} \leq V_{\omega vt}^P (X_v^0 + x_v) \quad \forall \omega, v, t \quad (37)$$

Unit commitment constraints (10)–(14) do not change in the power-based formulation. Equations (38), (39) limit the power output of thermal technologies. The total power output constraint is different depending whether it is a quick- or slow-start unit. Quick-start technologies \mathcal{G}^F are thermal generators that can startup/shutdown within one hour (i.e., $SU_{gk}^D = SD_g^D \leq 1$), while slow-start technologies \mathcal{G}^S are those with a SU/SD duration greater than one hour as well as a SU/SD capacity equal to the minimum power output (i.e., $SU_g = SD_g = \underline{P}_g$). Therefore, the total power output of slow-start technologies considers SU/SD trajectories (41), whereas (40) for quick-start technologies does not. For a better understanding of the modeling of quick- and slow-start technologies, the reader is referred to [18], [23]. The formulation presented here is based on the tight and compact formulation proposed in [14]. Furthermore, Morales-España *et al.* [18] has proven that the set of constraints (10)–(12) together with (38)–(41) is the tightest possible representation (i.e., convex hull) for the power-based model.

$$p_{\omega gt} + r_{\omega gt}^+ \leq (\bar{P}_g - \underline{P}_g) u_{\omega gt} - (\bar{P}_g - SD_g) z_{\omega g, t+1} + (SU_g - \underline{P}_g) y_{\omega g, t+1} \quad \forall \omega, g, t \quad (38)$$

$$p_{\omega gt} - r_{\omega gt}^- \geq 0 \quad \forall \omega, g, t \quad (39)$$

$$\hat{p}_{\omega gt} = \underline{P}_g (u_{\omega gt} + y_{\omega g, t+1}) + p_{\omega gt} \quad \forall \omega, g \in \mathcal{G}^F, t \quad (40)$$

$$\begin{aligned} \hat{p}_{\omega gt} = & \underbrace{\sum_{k=1}^{K_g} \sum_{i=1}^{SU_{gk}^D} P_{gki}^{SU} \delta_{\omega gk, (t-i+SU_{gk}^D+2)}}_{Startup \ trajectory} \\ & + \underbrace{\sum_{i=2}^{SD_g^D+1} P_{gi}^{SD} z_{\omega g, (t-i+2)}}_{Shutdown \ trajectory} + \underbrace{\underline{P}_g (u_{\omega gt} + y_{\omega g, t+1}) + p_{\omega gt}}_{Output \ when \ being \ up} \\ & \forall \omega, g \in \mathcal{G}^S, t \end{aligned} \quad (41)$$

ESS constraints for storage level (23) and storage level limits including reserve (24), (25) continue the same. Nevertheless, the logic to avoid charging and discharging at the same time (42), (43) is updated to consider the power output and charged power.

$$c_{\omega st} \leq (1 - \gamma_{\omega st}) \cdot (X_s^0 + \bar{X}_s) \quad \forall \omega, s, t \quad (42)$$

$$\hat{p}_{\omega st} \leq \gamma_{\omega st} \cdot (X_s^0 + \bar{X}_s) \quad \forall \omega, s, t \quad (43)$$

One of the main advantages of power-based formulation is that it allows to describe a more detailed set of constraints to represent the flexibility requirements, which are described in terms of power instead of energy. The proposed power-based equations in [14] ensure that reserves can be provided at any

time within the hour by guaranteeing that the reserve does not exceed the ramp-capability at τ -min (e.g., $\tau = 5$ min) and power-capacity limits at the end of the hour (i.e., 60 min). Therefore, (44), (45) guarantee that τ -min ramp capability is ensured for thermal technologies, while (46), (47) guarantee the power-capacity limit for both τ -min and at the end of the hour. These constraints have been defined for thermal generation units in [14]. However, ramping constraints in power-based models have not been defined for ESS in the literature before. This paper then proposes a set of constraints for flexibility requirements in power-based models. Fig. 4 shows different operating points and reserves for ESS at τ -min within hour t . Here, segments EA and AF must be below the ramp-capability limits τRU_s and τRD_s , as well as points E and F must be within the maximum and minimum power-capacity limit. Therefore, constraints (48)–(51) guarantee these conditions for all operating points of ESS in Fig. 4. Notice, that here it is important to highlight that (42), (43) avoid simultaneous charging and discharging.

$$\frac{\tau (p_{\omega gt} - p_{\omega g, t-1})}{60} + r_{\omega gt}^+ \leq \tau RU_g u_{\omega gt} \quad \forall \omega, g, t \quad (44)$$

$$-\frac{\tau (p_{\omega gt} - p_{\omega g, t-1})}{60} + r_{\omega gt}^- \leq \tau RD_g u_{\omega g, t-1} \quad \forall \omega, g, t \quad (45)$$

$$\frac{\tau p_{\omega gt} + (60 - \tau) p_{\omega g, t-1}}{60} + r_{\omega gt}^+ \leq (\bar{P}_g - \underline{P}_g) u_{\omega gt} \quad \forall \omega, g, t \quad (46)$$

$$\frac{\tau p_{\omega gt} + (60 - \tau) p_{\omega g, t-1}}{60} - r_{\omega gt}^- \geq 0 \quad \forall \omega, g, t \quad (47)$$

$$\begin{aligned} & \frac{\tau (\hat{p}_{\omega st} - \hat{p}_{\omega s, t-1})}{60} - \frac{\tau (c_{\omega st} - c_{\omega s, t-1})}{60} + r_{\omega st}^+ \\ & \leq \tau RU_s (X_s^0 + x_s) \quad \forall \omega, s, t \end{aligned} \quad (48)$$

$$\begin{aligned} & \frac{\tau (\hat{p}_{\omega st} - c_{\omega st}) + (60 - \tau) (\hat{p}_{\omega s, t-1} - c_{\omega s, t-1})}{60} + r_{\omega st}^+ \\ & \leq X_s^0 + x_s \quad \forall \omega, s, t \end{aligned} \quad (49)$$

$$\begin{aligned} & \frac{\tau (c_{\omega st} - c_{\omega s, t-1})}{60} - \frac{\tau (\hat{p}_{\omega st} - \hat{p}_{\omega s, t-1})}{60} + r_{\omega st}^- \\ & \leq \tau RD_s (X_s^0 + x_s) \quad \forall \omega, s, t \end{aligned} \quad (50)$$

$$\begin{aligned} & \frac{\tau (\hat{p}_{\omega st} - c_{\omega st}) + (60 - \tau) (\hat{p}_{\omega s, t-1} - c_{\omega s, t-1})}{60} - r_{\omega st}^- \\ & \geq -(X_s^0 + x_s) \quad \forall \omega, s, t \end{aligned} \quad (51)$$

III. SYSTEM FLEXIBILITY EVALUATION

As mentioned in the previous section, two main formulations are analyzed for GEP: the traditional energy-based (EB), and the power-based formulation (PB). We also analyze the traditional energy-based using SU/SD trajectories (EBs). Table I shows a summary with all the equations that define these models. All models include an hourly UC (either energy- or power-based) in order to consider operating constraints, involving those related to the power system flexibility (i.e., ramping and reserve constraints). In order to measure the quality of the obtained solution under real-time flexibility requirements, we carry out

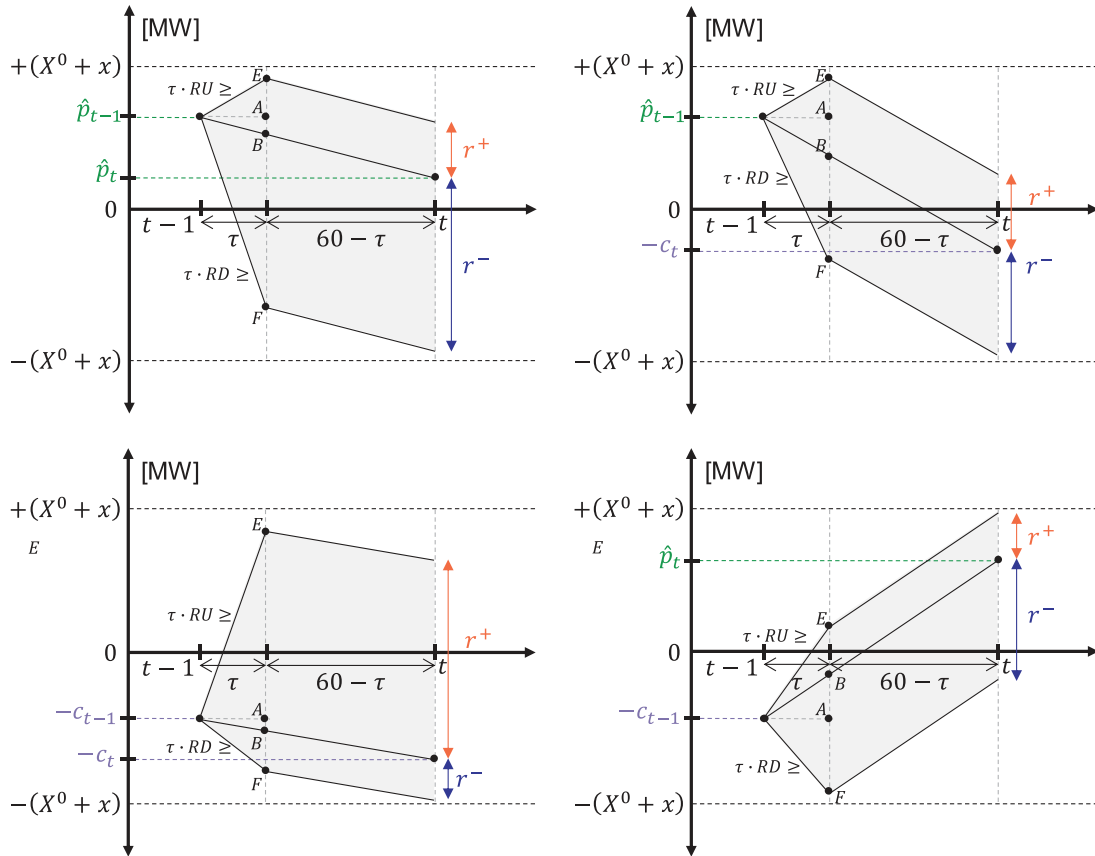


Fig. 4. Ramping constraints for ESS in the power-based model.

TABLE I
GEP-UC MODELS

Equations	EB	EBs	PB	SR-PB
Objective function	(1)		(30)	
System constraints	(2)-(5)		(4)-(5), (31)-(34)	
Investment constraints	(6),(7)-(8),(9)		(6), (35)-(36),(37)	
UC constraints	(10)-(14)			
Thermal unit constraints	(15)-(18)		(38)-(39)	
Total output thermal technologies	(19)	(20)	(40)-(41)	
ESS constraints	(21)-(25)		(23)-(25),(43)-(42)	
Constraints for flexibility requirements ($\tau = 5\text{min}$)	(26)-(29)		(44)-(51)	
Integer variables	$u_{\omega gt}, y_{\omega gt}, z_{\omega gt}, \gamma_{\omega st}, \delta_{\omega gkt}, x_j$		Stage 1a: x_j Stage 1b: $u_{\omega gt}, y_{\omega gt}, z_{\omega gt}, \gamma_{\omega st}, \delta_{\omega gkt}$	

an evaluation of investment and operational decisions through a simulation using the same scenarios as in the GEP-UC hourly optimization (in-sample simulation). This evaluation allows us to establish the problems associated to each formulation rather than those associated to the uncertainty representation by itself. The complete procedure to calculate investment decisions and ex-post real-time evaluation is shown in Fig. 5 (top). During stage 1, the investment and hourly UC schedule are optimized solving the formulations shown in Section II. Then, investment,

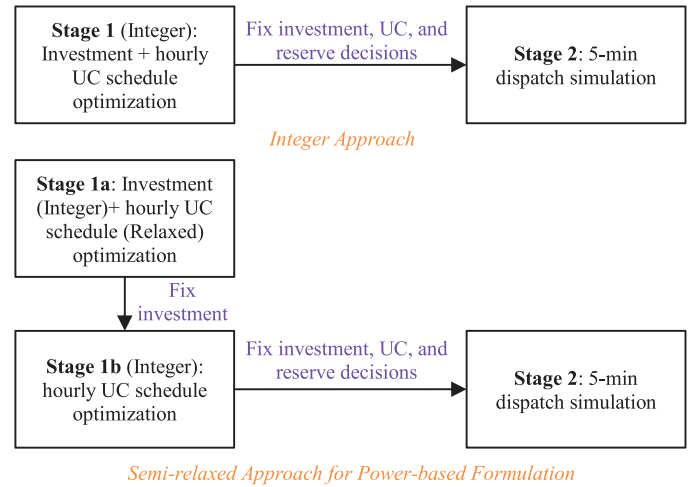


Fig. 5. Stage sequence for integer (top) and semi-relaxed (bottom) approaches.

commitment, and reserve decisions are fixed. Stage 2 tests the results through a real-time simulation model, using a 5-min optimal dispatch (emulating real-time markets as in [9]) in order to evaluate the GEP-UC solution. Dispatch decisions (e.g., production, charge/discharge) obtained in stage 2 are called redispaches, allowing us to evaluate the deviations with respect

to the stage 1. This is called the *integer approach*. In addition, we proposed a *semi-relaxed approach* for the power-based formulation, which is shown in Fig. 5 (bottom). Here we split stage 1 in two. First, the stage 1a solves the power-based formulation considering integer investment decisions and continuous UC decisions ($u_{\omega gt}, y_{\omega gt}, z_{\omega gt}$). This approximation allows to solve the GEP problem much faster. Then investment decisions are fixed in stage 1b, where the power-based formulation is solved considering integer UC decisions. Once again, investment, unit commitment, and reserve decisions are fixed to simulate a 5-min optimal dispatch.

IV. CASE STUDIES

To evaluate the performance of the different approaches, we use two case studies: a modified IEEE 118-bus test system and a stylized Dutch power system in target year 2040. Input data for both case studies is available online at [27], including the 5-min demand and renewable production profiles. Both case studies are solved considering a green-field investment approach (i.e., no initial capacity) for thermal generation and ESS investment, while the vRES capacity is predefined.

The modified IEEE 118-bus test system is described in Morales-España [28] for a time span of 24 h. This system was originally conceived for UC problems and it has 118 buses, 186 transmission lines, 91 loads, 54 slow-start thermal technologies, 10 quick-start technologies, and three buses with wind production. Nevertheless, we adapt this case study for GEP problems. Thermal unit investments are allowed in buses where there was a unit connected in the initial UC problem. In addition, ESS investment decisions are available in three types of technologies (PSH, CAES, and Li-ION) for buses with renewable production. The total (5-min) load average is 3578.6 MW, it has a peak of 5117.5 MW and a minimum of 1435.4 MW.

The stylized Dutch system case study for year 2040 is mainly based on the information available in the *Ten Year Network Development Plan 2018* [29] (e.g., hourly demand profile, renewable capacity, technical characteristics and available technologies). However, the wind and solar profiles were taken from [30], [31] since this information is not available in [29]. Instead of solving 8760 h for the whole year, we have selected four representative weeks using the proposed method in [32] and k-medoids clustering technique [33]. Other authors [34], [35] have proposed different approaches to select the representative periods (e.g., weeks or days) that are compatible with the proposed GEP-UC models in this paper. Each representative week is considered as one scenario in the optimization problem, and the scenario probability is obtained from the clustering process. For investment decisions, four different thermal generation technologies are considered, Combined Heat and Power (CHP), combined cycle gas turbine (CCGT), open cycle gas turbine (OCGT), and Light Oil (Oil). Moreover, three ESS (PSH, CAES, Li-ION) technologies are considered for investment decisions.

For each case study, four different models are implemented: traditional energy-based (EB), energy-based including SU/SD power trajectories (EBs), the proposed power-based formulation (PB), and the semi-relaxed power-based formulation (SR-PB).

TABLE II
IEEE 118-BUS SYSTEM: PERFORMANCE FOR EACH FORMULATION

	Result	EB	EBs	PB	SR-PB
Stage 1	Total Cost [M\$]	10.15	9.29	8.94	8.96 [†]
	ESS Invest Cost [M\$]	0.43	0.35	0.19	0.17
	Therm. Invest Cost [M\$]	1.01	1.42	1.17	1.24
	Operating Cost [M\$]	8.71	7.52	7.58	7.55 [†]
	CO2 emissions [ton]	63.11	53.06	53.98	53.74
	Curtailment [%]	5.76	4.18	0.73	0.70
Stage 2	CPU Time [s]	10717	6767	4478	500
	Operating Cost [M\$]	8.22	7.53	7.58	7.55
	Total Cost [M\$]	9.66	9.30	8.94	8.96
	CO2 emissions [ton]	59.31	52.48	53.95	53.71
	Curtailment [%]	0.00	0.00	0.60	0.62

[†]Values from Stage 1b.

TABLE III
TECHNOLOGY INVESTMENT DECISIONS [MW]

Technology	EB	EBs	PB	SR-PB
PSH	1250	1000	500	441
CAES	0	0	0	0
Li-ION	150	150	150	150
GAS	360	600	420	480
COAL	4380	6080	5030	5330
OIL	50	100	100	100

Table I shows the summary with all the implemented models. All models consider $\tau = 5$ min for constraints associated to flexibility constraints.

All optimizations were carried out using Gurobi 8.1 on an Intel-Core i7-4770 (64-bit) 3.4-GHz personal computer with 16 GB of RAM memory. The problems are solved until they reach an optimality tolerance of 0.1%.

V. RESULTS

A. Modified IEEE 118-Bus System

Table II shows the main results for each model. The total investment cost (ESS + Thermal) is higher in the classic EB model than the one obtained with the PB model. Generally, increasing the investments lowers operating cost. Nevertheless, here we obtain a counterintuitive result. Even though the classic EB model invests more (6%), the operating cost is worse than the one in the PB model (15%). Moreover, the CO2 emissions and curtailment are also higher in the classic EB model, despite its higher capacity in clean ESS and lower capacity in thermal technologies. This is also a counterintuitive result, because at a first glance, less thermal generation should pollute less, and more storage should allocate more renewables. However, this result is related to how the technology mix is selected in each model. Therefore, it is not only a matter of how much the model invests, it is also a matter of how the technology mix is selected, see Table III. For instance, although the total coal capacity is higher in the proposed PB model, the actual total coal production is lower (7%) than the one in the classic EB model, see Table IV. This is compensated by a higher use of wind, gas (that have less CO2 emission factor) and oil, which overall results in less CO2 emissions. As mentioned in Section II-B. the PB model

TABLE IV
TECHNOLOGY PRODUCTION DECISIONS [MWh]

Technology	EB	EBs	PB	SR-PB
PSH	7352	5944	2449	2019
CAES	0	0	0	0
Li-ION	1053	1003	1035	1033
GAS	494	2719	2482	2680
COAL	67540	63939	62913	62570
OIL	52	900	950	900
WIND	18880	19196	19887	20018

equations allow to schedule the thermal technologies in a way that correctly represents the requirements and actual availability of system's flexibility, such as the load ramps. The results show the benefits of accurately considering the flexibility requirements and of correctly modelling the flexibility capabilities of the system by modelling in terms of power instead of energy.

The EBs model improves the classic EB model by including the SU/SD power-based ramps. In stage 1, the total cost in the EBs model is 8.5% lower than the classic EB model. However, it is still 4% higher than the PB model and with more curtailment (5.7 times). The EBs technology mix is also different, as it invests more in PHS and coal (Table III). And yet, the PB model allocates more wind with less ESS, see Table IV. Therefore, the PB model invests more efficiently due to the more accurate representation of flexibility requirements and capabilities of the power system.

Regarding the CPU time, the PB model is faster than its energy counterparts (2.4 and 1.5 times respectively). Nevertheless, for large-scale investment decision problems, the integer nature of the UC variables especially could make the problem intractable to solve. Therefore, the proposed SR-PB models aims at overcoming this situation. For instance, it solves the problem 9 times faster than the PB model and with only a 0.2% difference in the objective function. Moreover, the difference in the CO2 emissions is only 0.4%. The main difference appears in the curtailment (90%) due to the increase in the investment made by the SR-PB that allows to reduce the operating cost by increasing wind production. When the SR-PB and the EB are compared, it may be concluded that the even the semi-relaxed version of the power-based model (i.e., SR-PB) shows better performance than the discrete version of the energy-based models (i.e., EB and EBs). In other words, the SR-PB model has a lower total cost than the EB model, investing and operating with lower cost, while simultaneously solving 21+ times faster.

The results in Table II for the stage 2 are also showing interesting information: comparing the operating cost between stage 1 and 2, the classic EB shows a decrease of 6%, while in the other models remain almost the same. Moreover, the curtailment is also reduced from stage 1 to stage 2 in both energy-based models, while it remains almost the same in the power-based models. These results suggest that the obtained schedule in stage 1 with energy-based models leads to more redispatches in the technologies in stage 2. Fig. 6 illustrates this situation with the deviation with respect to the hourly thermal production obtained in stage 2 for each model. In both energy-based models, downward deviations are higher than upward deviations, which

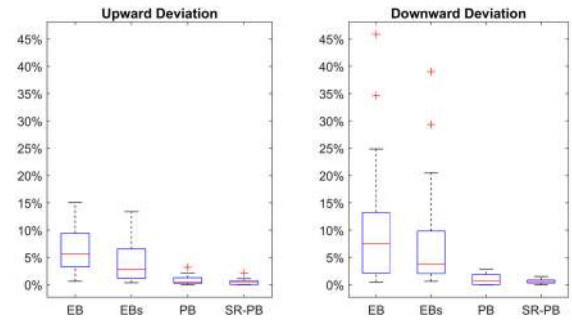


Fig. 6. Stage 2 deviation in scheduled thermal output.

TABLE V
IEEE 118-BUS SYSTEM: STAGE 2 – SENSITIVITY RESULTS

	Result	EB	EBs	PB	SR-PB
Stage 2	Operating Cost [M\$]	8.35	7.66	7.60	7.55
	Total Cost [M\$]	9.79	9.43	8.96	8.96
	CO2 emissions [ton]	59.89	52.71	54.04	53.73
	Curtailment [%]	1.99	0.98	0.62	0.13

explains why the operating cost is reduced from stage 1 to stage 2 in the classic EB model as well as the reduction on the curtailment for both energy-based models. The power-based models show deviations in both directions lower than 3%, which means that the hourly schedule (stage 1) is better fitted for the 5-min real-time operation (stage 2). This high deviation of the energy-based models is due to its intrinsic incapability to accurately represent the flexibility needs and capabilities. These conclusions are aligned with those in [9] where different case studies were carried out disregarding investment decisions.

Notice that ESS plays an important role in the reschedules made in stage 2. Therefore, we run a sensitivity case in which the State-of-Charge (SoC) at the end of each hour is a lower bound for the ESS in the stage 2. This limits the reschedules made in this stage, increasing the operating cost. Table V shows that situation, where with this additional constraint the operating cost, CO2 emissions and curtailment are higher than in the base case. It is important to highlight that in this sensitivity case energy-type models cannot reduce the curtailment to zero as it was in the base case. Therefore, the flexibility provided by the ESS was partly responsible for the reduction of the curtailment between stage 1 and 2 in this type of models. Fig. 7 shows the SoC in the batteries during stage 2 for the base case and the sensitivity case.

The difference between both results in each model shows how the energy-type models were taking advantage of the ESS to reduce the operating cost in stage 2 at the cost of more rescheduling in the thermal technologies.

B. Stylized Dutch System

Table VI shows the results for a stylized Dutch power system. The main conclusions drawn from the previous case study remain valid. That is, the classic EB model obtains the most expensive investment, and the operating cost is also the highest, while also resulting in the highest CO2 emissions. The amount of

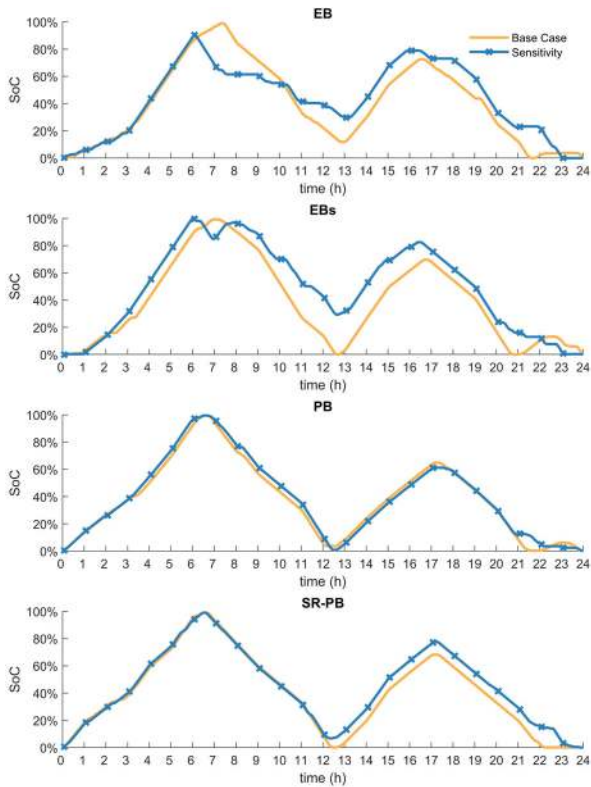


Fig. 7. Battery SoC in Stage 2 obtained for each model.

TABLE VI
STYLIZED DUTCH SYSTEM: PERFORMANCE FOR EACH FORMULATION

	Result	EB	EBs	PB	SR-PB
Stage 1	Total Cost [M\$]	73.18	70.39	68.14	68.16 [†]
	ESS Invest Cost [M\$]	13.47	11.15	10.53	10.88
	Therm. Invest Cost [M\$]	13.79	14.12	13.43	13.47
	Operating Cost [M\$]	45.92	45.12	44.18	43.81 [†]
	CO2 emissions [kton]	112.10	98.06	89.46	88.77
	Curtailment [%]	44.72	45.47	45.46	45.34
Stage 2	Operating Cost [M\$]	45.76	46.61	44.90	44.52
	Total Cost [M\$]	73.02	71.88	68.86	68.87
	CO2 emissions [kton]	107.73	100.01	94.29	93.44
	Curtailment [%]	47.88	48.35	48.34	45.39

[†]Values from Stage 1b.

ESS invested in the EB model is also the highest, hence allowing it to obtain less curtailment than PB in the stage 2. Nevertheless, still the PB model results in the lowest total cost in both stages and solves the GEP problem faster than EB. In addition, the SR-PB further reduces the CPU time without losing accuracy in the results. Therefore, modeling flexibility requirements with the PB model leads to a better solution than the classic EB model. In addition to the base case shown in Table VI, Table VII shows a sensitivity where ramp capabilities of thermal technologies are twice than before, i.e., thermal technologies are now much more flexible. As the flexibility of the thermal resources increases, the difference between energy-based and power-based models decreases. For instance, the difference between the EB the PB models changes from 7.4% to 4.3%. Therefore, if the power

TABLE VII
STYLIZED DUTCH SYSTEM: SENSITIVITY TO RAMP CAPACITY

	Result	EB	EBs	PB	SR-PB
Stage 1	Total Cost [M\$]	70.51	67.93	67.60	67.61 [†]
	ESS Invest Cost [M\$]	13.35	10.97	10.66	10.74
	Therm. Invest Cost [M\$]	13.47	13.47	13.43	13.47
	Operating Cost [M\$]	43.69	43.49	43.51	43.40 [†]
	CO2 emissions [kton]	103.10	90.84	88.46	88.17
	Curtailment [%]	44.32	45.22	45.16	45.19
	CPU Time [s]	142	130	100	43
Stage 2	Operating Cost [M\$]	44.37	45.92	44.25	44.21
	Total Cost [M\$]	71.19	70.36	68.34	68.42
	CO2 emissions [kton]	100.76	94.35	93.07	93.07
	Curtailment [%]	44.62	45.30	45.24	45.28

[†]Values from Stage 1b.

system does not have ramp problems, i.e., flexibility is not a problem in general, the difference between energy-based and power-based models is less significant. However, if flexibility is a limited resource and needs to be correctly managed, then the power-based models are the right option to obtain the capacity expansion planning for the system.

VI. CONCLUSION

This paper proposes a power-based model to determine the GEP, including energy storage technologies. The proposed power-based model uses the installed investments more efficiently and more effectively as 1) it represents the reality of flexibility requirements of the power system more adequately, and 2) it adequately exploits the flexibility capabilities of the system. That is, the decisions made with the power-based model simultaneously yield lower investment costs, operating cost, CO2 emissions, and renewable curtailment with respect to the energy-based model. This is mainly because the energy-based model overestimates flexibility capabilities, failing to capture the flexibility requirements such as load and vRES ramps even in a deterministic approach (i.e., without uncertainty on demand, or renewable production). Moreover, the advantages of the power-based approach could become much more significant considering uncertainty [9]. Therefore, correctly modeling the system flexibility changes the optimal expansion capacity decisions. For instance, the power-based model obtains less total investment (6–12%) because it is more accurate in the representation of ramping characteristics for generation resources (e.g., thermal technologies and ESS), which leads to less operating cost (2–8%) in the real-time validation. In addition, the power-based model has computational advantages in terms of CPU time. The results show that the power-based model is 2 to 4 times faster than the energy-based model. We also have demonstrated that the semi-relaxed power-based model is even faster (10 to 21 times) without losing accuracy in the results compared with the non-relaxed power-based model (less than 0.2% objective function error). This is relevant for applications with large-scale long-term capacity expansion planning problems where relaxed models are more often used due to computational power limitations.

The results show an important insight for ISOs because, even without uncertainty, the current energy-based models impose

more rescheduling in the real-time operation than the power-based models. For planning authorities this is also important because decisions made with power-based models lead to a generation technology mix that is better adapted to real-time system operation.

Finally, the proposed power-based UC model relies on available data in terms of power trajectories instead of energy trajectories, i.e., demand and renewable profiles. Forecasting power profiles, thus having higher quality on ramping information, is an interesting topic that could be addressed in future research.

REFERENCES

- [1] B. F. Hobbs, "Optimization methods for electric utility resource planning," *Eur. J. Oper. Res.*, vol. 83, no. 1, pp. 1–20, May 1995.
- [2] V. Oree, S. Z. Sayed Hassen, and P. J. Fleming, "Generation expansion planning optimisation with renewable energy integration: A review," *Renew. Sustain. Energy Rev.*, vol. 69, pp. 790–803, Mar. 2017.
- [3] H. Saboori and R. Hemmati, "Considering carbon capture and storage in electricity generation expansion planning," *IEEE Trans. Sustain. Energy*, vol. 7, no. 4, pp. 1371–1378, Oct. 2016.
- [4] K. Poncelet, E. Delarue, D. Six, J. Duerinck, and W. D'haeseleer, "Impact of the level of temporal and operational detail in energy-system planning models," *Appl. Energy*, vol. 162, pp. 631–643, Jan. 2016.
- [5] N. E. Koltsaklis and A. S. Dagoumas, "State-of-the-art generation expansion planning: A review," *Appl. Energy*, vol. 230, pp. 563–589, Nov. 2018.
- [6] B. Hua, R. Baldick, and J. Wang, "Representing operational flexibility in generation expansion planning through convex relaxation of unit commitment," *IEEE Trans. Power Syst.*, vol. 33, no. 2, pp. 2272–2281, Mar. 2018.
- [7] B. S. Palmintier and M. D. Webster, "Impact of operational flexibility on electricity generation planning with renewable and carbon targets," *IEEE Trans. Sustain. Energy*, vol. 7, no. 2, pp. 672–684, Apr. 2016.
- [8] B. F. Hobbs and S. S. Oren, "Three waves of U.S. reforms: Following the path of wholesale electricity market restructuring," *IEEE Power Energy Mag.*, vol. 17, no. 1, pp. 73–81, Jan. 2019.
- [9] G. Morales-España, L. Ramírez-Elizondo, and B. F. Hobbs, "Hidden power system inflexibilities imposed by traditional unit commitment formulations," *Appl. Energy*, vol. 191, pp. 223–238, Apr. 2017.
- [10] R. Loulou and M. Labriet, "ETSAP-TIAM: The TIMES integrated assessment model Part I: Model structure," *Comput. Manag. Sci.*, vol. 5, no. 1–2, pp. 7–40, Feb. 2008.
- [11] "NREL: Energy Analysis - Regional Energy Deployment System (ReEDS) Model," 2016. [Online]. Available: <http://www.nrel.gov/analysis/reeds/>. [Accessed: Apr. 12, 2016].
- [12] "Resource Planning Model | Energy Analysis | NREL," 2016. [Online]. Available: <https://www.nrel.gov/analysis/models-rpm.html>. [Accessed: Jan. 30, 2018].
- [13] W. Lise, J. Sijm, and B. F. Hobbs, "The impact of the EU ETS on prices, profits and emissions in the power sector: Simulation results with the COMPETES EU20 model," *Environ. Resour. Econ.*, vol. 47, no. 1, pp. 23–44, Apr. 2010.
- [14] G. Morales-España, A. Ramos, and J. Garcia-Gonzalez, "An MIP formulation for joint market-clearing of energy and reserves based on ramp scheduling," *Power Syst. IEEE Trans.*, vol. 29, no. 1, pp. 476–488, Jan. 2014.
- [15] G. Morales-España, R. Baldick, J. García-González, and A. Ramos, "Power-capacity and ramp-capability reserves for wind integration in power-based UC," *IEEE Trans. Sustain. Energy*, vol. 7, no. 2, pp. 614–624, Apr. 2016.
- [16] X. Guan, F. Gao, and A. J. Svoboda, "Energy delivery capacity and generation scheduling in the deregulated electric power market," *IEEE Trans. Power Syst.*, vol. 15, no. 4, pp. 1275–1280, Nov. 2000.
- [17] Y. Yang, J. Wang, X. Guan, and Q. Zhai, "Subhourly unit commitment with feasible energy delivery constraints," *Appl. Energy*, vol. 96, pp. 245–252, Aug. 2012.
- [18] G. Morales-España, C. Gentile, and A. Ramos, "Tight MIP formulations of the power-based unit commitment problem," *Spectr.*, vol. 37, no. 4, pp. 929–950, Oct. 2015.
- [19] G. Strbac *et al.*, "Opportunities for energy storage: Assessing whole-system economic benefits of energy storage in future electricity systems," *IEEE Power Energy Mag.*, vol. 15, no. 5, pp. 32–41, Sep. 2017.
- [20] J. Meus, K. Poncelet, and E. Delarue, "Applicability of a clustered unit commitment model in power system modeling," *IEEE Trans. Power Syst.*, vol. 33, no. 2, pp. 2195–2204, Mar. 2018.
- [21] G. Morales-España and D. A. Tejada-Arango, "Modelling the hidden flexibility of clustered unit commitment," *IEEE Trans. Power Syst.*, vol. 34, no. 4, pp. 3294–3296, Jul. 2019.
- [22] G. Morales-España, J. M. Latorre, and A. Ramos, "Tight and compact MILP formulation for the thermal unit commitment problem," *IEEE Trans. Power Syst.*, vol. 28, no. 4, pp. 4897–4908, Nov. 2013.
- [23] C. Gentile, G. Morales-España, and A. Ramos, "A tight MIP formulation of the unit commitment problem with start-up and shut-down constraints," *EURO J. Comput. Optim.*, pp. 1–25, Apr. 2016.
- [24] G. Morales-España, J. M. Latorre, and A. Ramos, "Tight and compact MILP formulation of start-up and shut-down ramping in unit commitment," *Power Syst. IEEE Trans.*, vol. 28, no. 2, pp. 1288–1296, May 2013.
- [25] I. Momber, G. Morales-España, A. Ramos, and T. Gómez, "PEV storage in multi-bus scheduling problems," *IEEE Trans. Smart Grid*, vol. 5, no. 2, pp. 1079–1087, Mar. 2014.
- [26] R. Philipsen, G. Morales-España, M. de Weerd, and L. de Vries, "Trading power instead of energy in day-ahead electricity markets," *Appl. Energy*, vol. 233–234, pp. 802–815, Jan. 2019.
- [27] D. A. Tejada-Arango, "Case studies for power-based capacity expansion planning: datejada/PB-CEP," Dec. 21, 2018. [Online]. Available: <https://github.com/datejada/PB-CEP>. [Accessed: 21-Dec-2018].
- [28] G. Morales-España, "Unit Commitment: Computational performance, system representation and wind uncertainty management," Doctoral thesis, Universidad Pontificia Comillas, KTH Royal Institute of Technology, and Delft University of Technology, 2014.
- [29] ENTSO-E, "Ten Year Network Development Plan 2018," 2018. [Online]. Available: <https://tyndp.entsoe.eu/>. [Accessed: Dec. 21, 2018].
- [30] I. Staffell and S. Pfenninger, "Using bias-corrected reanalysis to simulate current and future wind power output," *Energy*, vol. 114, pp. 1224–1239, Nov. 2016.
- [31] S. Pfenninger and I. Staffell, "Long-term patterns of European PV output using 30 years of validated hourly reanalysis and satellite data," *Energy*, vol. 114, pp. 1251–1265, Nov. 2016.
- [32] D. A. Tejada-Arango, M. Domeshek, S. Wogrin, and E. Centeno, "Enhanced representative days and system states modeling for energy storage investment analysis," *IEEE Trans. Power Syst.*, vol. 33, no. 6, pp. 6534–6544, Nov. 2018.
- [33] H.-S. Park and C.-H. Jun, "A simple and fast algorithm for K-Medoids clustering," *Expert Syst. Appl.*, vol. 36, no. 2, Part 2, pp. 3336–3341, Mar. 2009.
- [34] S. Pineda and J. M. Morales, "Chronological time-period clustering for optimal capacity expansion planning with storage," *IEEE Trans. Power Syst.*, vol. 33, no. 6, pp. 7162–7170, Nov. 2018.
- [35] M. Sun, F. Teng, X. Zhang, G. Strbac, and D. Pudjianto, "Data-driven representative day selection for investment decisions: A cost-oriented approach," *IEEE Trans. Power Syst.*, vol. 34, no. 4, pp. 2925–2936, Jul. 2019.

Diego A. Tejada-Arango (M'11) received the B.Sc. degree in electrical engineering from the Universidad Nacional, in Medellín, Colombia, in 2006, the M.Sc. degree in electrical engineering from the Universidad de Antioquia, in Medellín, Colombia with the GIMEL Group, in 2013, the master's degree in engineering systems modeling from Universidad Pontificia Comillas, in Madrid, Spain, in 2017, and the Ph.D. degree from the Universidad Pontificia Comillas, Spain, in 2019. His research interests include generation expansion planning as well as planning and operation of electric energy systems.

Germán Morales-España (S'10–M'14–SM'18) received the B.Sc. degree in electrical engineering from the Universidad Industrial de Santander, Bucaramanga, Colombia, in 2007, the M.Sc. degree from the Delft University of Technology (TUDelft), Delft, The Netherlands, in 2010, and the Joint Ph.D. degree from the Universidad Pontificia Comillas, Madrid, Spain, the Royal Institute of Technology, Stockholm, Sweden, and TUDelft, Delft, The Netherlands, in 2014. Since 2017, he has been with the Energy research Centre of the Netherlands (ECN part of TNO), Energy Transition Studies, as a Scientific Researcher. His research interests include planning, operation, economics, and reliability of electric systems and sector coupling.

Sonja Wogrin (M'13–SM'19) received the Dipl. Ing. degree in technical mathematics from the Graz University of Technology, Austria, in 2008, the M.S. degree in computation for design and optimization from the Massachusetts Institute of Technology, Cambridge, MA, USA, in 2008, and the Ph.D. degree from the Universidad Pontificia Comillas, Spain, in 2013, where she is now an Associate Professor. Her research interests lie within the area of decision support systems in the energy sector, energy storage, optimization and modeling, and, in particular, the generation capacity expansion problem.

Efraim Centeno received the degree in industrial engineering and the Ph.D. degree in industrial engineering from the Universidad Pontificia Comillas de Madrid, Madrid, Spain, in 1991 and 1998, respectively. He is a Research Staff at the Instituto de Investigación Tecnológica (IIT), Universidad Pontificia Comillas. His areas of interest include the planning and development of electric energy systems.